Impacts of Climate Change on Autumn North Atlantic Wave Climate

Will Perrie, Lanli Guo, Zhenxia Long, Bash Toulany

Fisheries and Oceans Canada, Bedford Institute of Oceanography, Dartmouth, NS

Abstract

In this study, the impact of greenhouse gas (GHG)-induced global warming on the means and extremes of the North Atlantic (NA) ocean wave climate, and associated storm climate are investigated using outputs derived from the WAVEWATCH-III (hereafter WW3) wave model and dynamically downscaled outputs from Canadian Regional Climate Model CRCM, driven by the IPCC 20th Century (20C3M) (1970-1999) and SRES A1B scenario emissions (2040-2069) estimates from the Coupled Global Climate Model CGCM3.1 (T47). WW3 is driven by 6 hourly sea surface wind fields from CRCM downscaled outputs *hereafter*. Compared with current wave climatology, increases in significant wave heights (SWH) in the northeast NA, with decreases in the NA mid-latitudes are found to be associated with storm climate change over these areas.

1. Introduction

Waves are a main climate factor affecting coastal regions. Over recent decades, reports of extreme wave heights encountered in individual severe storms have increased public and scientific concerns on how storm activity, waves and storm surge might change under global warming. However, because of limited confidence in model projections for changes related to the ocean wave climate, this topic received minimal attention in IPCC AR4. The dominant source of uncertainty in regional wave projections is the wind fields as generated by global projections. This uncertainty and its impacts on waves needs to be resolved [*Hemer et al.*, 2010].

Storms impact the upper ocean. Climate change potentially affects mean sea level and meteorological regimes (storminess, cyclone intensities and trajectories). *Bacon and Carter* [1993] investigated the connections between wave height changes and north–south atmospheric pressure gradients in the North Atlantic. Changes in storm activity and global wind patterns may affect the wave climate [*Kushnir et al.*, 1997; *Wang and Swail*, 2001]. By using the CGCM2's outputs, *Wang and Swail* [2006] investigated climate change related to wave heights through statistical analysis. The purpose of this study is to use dynamical downscaling to analyze possible changes in SWH (significant wave height), winds and storms under global warming over the North Atlantic. A two-step automated storm detection and tracking system is used, adapted from *Long et al.* [2009].

2. Model and data

2.1 Atmospheric model

In this study, CRCM version 3.7.1 [*Tanguay et al.*, 1990; *Caya and Laprise*, 1999] is implemented for the computational domain shown in Figure 1, which covers much of the North American continent, the North Atlantic Ocean, and part of Western Europe. Initial and lateral boundary conditions are taken from CGCM3 (T47) outputs, with horizontal resolution of ~3.75°. To represent the present climate, a 30-year (1 January

1970 to 31 December 1999) simulation is performed; the future climate is taken from 2040–69 of CGCM3 simulations, following the IPCC SRES A1B scenario.

2.2 Wave Model

A third-generation WW3 spectral wave model [*Tolman*, 2009] is used, with default settings based on deep water physics, and a linear bottom dissipation parameterization following WAMDI [1988]. The model domain is shown in Figure 3, focusing on the North Atlantic Ocean (20°N –70°N, 82°W –18°E). The outer boundary of the domain is closed. Thus, the local wave climate is due to the atmospheric forcing within our study region; no swell from outside this domain can affect the results. The Wave model grid spacing is 0.5° × 0.5°. Six-hourly 10 m wind fields (45 km) from CRCM are interpolated to the WW3 grid (0.5° × 0.5°) using quadratic interpolation. Simulations are August 30 to October 31 for each year during 1970-1999 and 2040-2069. Three-hourly output wave fields are archived.

2.3 ERA40 wave reanalysis

The ERA40 wave dataset is used for comparisons with the ocean wave climate from WW3 model results. This reanalysis was produced by ECMWF's Integrated Forecasting System, which includes variational data assimilation.

3. Current Climate Results

3.1 Wind fields from the atmospheric model

Figure 1 depicts the 6-hourly autumn winds (September and October) averaged over 30 years (1970-1999) for NCEP, ERA40 and CRCM, and 10years (1991-2000) for QSCAT/NCEP blended ocean winds. The maximum wind appears at high latitudes in all these data. Figure 1a is the QSCAT/NCEP blended winds, containing higher spatial resolution QuikSCAT wind data than NCEP and ERA40 reanalysis data. Comparable results for CRCM data (Figure 1d), again reflect the dominant North Atlantic 10m winds, especially over high-latitude areas. Spatial details in QSCAT/NCEP blended winds, for example the maxima near Greenland and Gulf of St. Lawrence coastal areas are reproduced by CRCM. The region with winds above ~10 m/s over the Northeast Atlantic is consistent with dominant results suggested by QSCAT/NCEP data. Figures 1b-1c show that ERA40 winds are underestimated, and NCEP winds slightly overestimated.

Figure 2 presents the extreme winds, defined as the average of the highest 10% of the 6 hourly 10m winds for each autumn (hereafter Wtop10), following *Sasaki et al.* [2005]. The most prominent feature in QSCAT/NCEP (Figure 2a) is the strong winds occurring over high latitudes, with the highest winds over Greenland's southeast coast. Although CRCM has the same patterns as QSCAT/NCEP, ERA40 and NCEP are too coarse to get the small spatial details over Greenland's southeast coast. As in Figure 1, Wtop10 is underestimated by ERA40, and overestimated by NCEP data (Figures 2b~2c).

3.2 Wave climate

Seasonal mean of 6-hourly significant wave heights (SWH) for the current climate are shown in Figures 3a~3b for ERA40 and CRCM winds. For the boreal fall (September

~ October), the SWH climate is characterized by high waves in high-latitudes of the Northeast Atlantic. The maximum seasonal mean SWH is ~4 m in ERA40 data. Figure 3b shows that WW3 can simulate the typical SWH climate in the ERA40 data, although with stronger wave heights than ERA40, reflecting the winds in these two data sets. Mean wave direction, and mean wave period (Tm) are additional important integral wave parameters. Mean wave directions are given in degrees and are defined using the meteorological convention where zero means "coming from North" and "90"coming from East". Figures 3c~3d give the mean wave directions showing that WW3 produces similar wave direction patterns as ERA40, except the simulated wave directions are more eastward over the east North Atlantic. Figure 3e shows the mean Tm climate in ERA40, featuring a large region of long wave periods in the east North Atlantic. Comparisons with ERA40 show that although WW3 (Figure 3f) tends to overestimate Tm over the east coastal area, and underestimate Tm over the west coastal area, it can generally reproduce the same climatology as ERA40. Autumn extreme SWH values, defined as the average of the highest 10% of the 6 hourly SWH for each autumn are shown in Figures 3g~3h (hereafter Htop10). The simulated maximum of Htop10 (from WW3) is around 7.5m, which is stronger than the ERA40 estimate of 5.5m.

3.3 storm climates

Climate change effects on waves should depend on changes to the storm climate. The storm track density is calculated by counting the number of storm tracks that pass through each 1000 km×1000 km box in autumn months (September ~ October), averaged over 30 years (1970-1999). In terms of the annual mean distribution, the highest frequency of storm events tends to occur over Greenland's southeast area, as suggested by ERA40 and NCEP reanalysis data (Figures 4a~4b). Compared with reanalysis data, the storm track frequency is underestimated by CGCM3 over the southeast tip of Greenland and along the east coast of North America (Figure 4c). Track density simulations from CRCM are given in Figure 4d. Although CRCM seems to overestimate the storm density compared to ERA40 and NCEP over high latitudes, its track maximum is located over the southeast tip of Greenland, which is consistent with the results of reanalysis data. Like CGCM3, the storm density in CRCM appears to be underestimated along the east coast of North America, compared to reanalysis data.

Figure 5 gives the spatial storm track frequency distribution of intense cyclones based on minimum MSLP less than 970 hPa. ERA40 and NCEP (Figures 5a~5b) give the same phenomenon, suggesting that most intense storms occur over high latitudes, especially over the area southwest of Iceland. Compared with reanalysis data, CGCM3 (Figure 5c) can capture the general characteristics of the intense storm distribution, but underestimates the storms occurring south of Iceland and overestimates the Labrador Sea storms. The CRCM results (Figure 5d) are improved compared to CGCM3, particularly over the area southwest of Iceland, but overestimates occur for the Labrador Sea storms.

4. Climate change results

Figure 7 shows the impacts of climate change on the wave climate. Under the IPCC A1B scenario, slight increases of mean SWH appear over the Northeast Atlantic, with decreases in the subtropical North Atlantic (Figure 7a). Similar results were found by *Wang and Swail* [2006] using only the CGCM2 projections. Figure 7b shows changes in

the extreme SWH that are similar to changes in the mean SWH except the largest SWH increases appear over the Northeast Atlantic. As driving fields, winds display the similar change patterns as SWH. Figure 6 indicates the difference in mean and 10% strongest 6-hourly winds between future GHG-warmed climate and present climate, as simulated by CRCM. Compared with the current climate, the winds (especially strong winds) decrease over the midlatitudes and increase over the Northeast Atlantic, influencing the wave climate. In the climate change simulation, mean wave directions increase over the Northeast Atlantic (more westerly) and decrease over the Southeast Atlantic (more easterly) relative to the current climate; the significance level is above 90% with the Student's t-test (Figure 7c). Figure 7d shows that Tm is slightly longer over the Northeast Atlantic and shorter over the subtropical North Atlantic, although these results are not statistically significant.

Consistent with SWH decreases over the subtropical North Atlantic, an associated storm density decrease also occurs, which is related to changes in the atmospheric circulation. Figure 8 show the impacts of climate change on the storm density. The light shading indicates 90% significance level with the Student's t-test. Under the warming climate scenario, significant increases in mean and intense (minimum sea level pressure ≤ 970 hPa) storm results appear in the area to the north of ~50^{o}N, and in the Northeast Atlantic, respectively; decreases are indicated in the subtropical North Atlantic for both of CGCM3 and CRCM.

5. Conclusions

The possible influence of climate change on North Atlantic waves and storm climate are studied using outputs from WW3 wave model and dynamically downscaled outputs and winds from the Coupled Regional Climate Model (CRCM). For the current climate, CRCM and WW3 models can capture general characteristics of waves, winds and storm tracks suggested by reanalysis data. Compared with the current literature, significant increases of SWH in the northeast North Atlantic, matched by significant decreases in the mid-latitude North Atlantic, are found to be associated with changes in the winds and storm climate over these areas.

Acknowledgements

We want to thank DFO's Climate Change Science Initiative (CCSI) and the Canadian Panel on Energy Research and Development (PERD) for funding to support this work.

References

Bacon, S., and D. J. T. Carter (1993), A connection between mean wave height and atmospheric pressure gradient in the North Atlantic, *Int. J. Climatol*., *13*, 434–436.

Caya, D., and R. Laprise (1999), A semi-implicit semi-lagrangian regional climate model: The Canadian RCM, *Mon. Wea. Rev.*, **127**, 341-362.

Hemer, M. A., J. A. Church, and J. R. Hunter (2010), Variability and trends in the directional wave climate of the Southern Hemisphere, *Int. J. Climatol.*, *30*, 475–491, doi: 10.1002/joc.1900.

Kushnir, Y., V. J. Cardone, J. G. Greenwood, and M. A. Cane (1997), The recent increase in North Atlantic wave heights, *J. Clim*., *10*, 2107–2113.

Long, Z., W. Perrie, J. Gyakum, R. Laprise, and D. Caya (2009), Scenario changes in the climatology of winter midlatitude cyclone activity over eastern North America and the Northwest Atlantic, *J. Geophys. Res.*, *114*, D12111, doi:10.1029/2008JD010869.

Sasaki, W., S. I. Iwasaki, T. Matsuura, and S. Iizuka (2005), Recent increase in summertime extreme wave heights in the western North Pacific, *Geophys. Res. Lett.*, *32*, L15607, doi:10.1029/2005GL023722.

Tanguay, M., A. Robert, and R. Laprise (1990), A semi-implicit semi-lagrangian fully compressible regional forecast model, *Mon. Wea. Rev.*, **118,** 1970–1980.

Tolman, H. L. (2009), User manual and system documentation of WAVEWATCH III version 3.14, *Tech. Note 276*, 194 pp.

Wang, X. L., and V. R. Swail (2001), Changes of extreme wave heights in Northern Hemisphere oceans and related atmospheric circulation regimes, *J. Clim.*, *14*, 2204–2221.

Wang, X. L., and V. R. Swail (2006), Climate change signal and uncertainty in projections of ocean wave heights, *Clim. Dyn.*, *26*, 109-126.

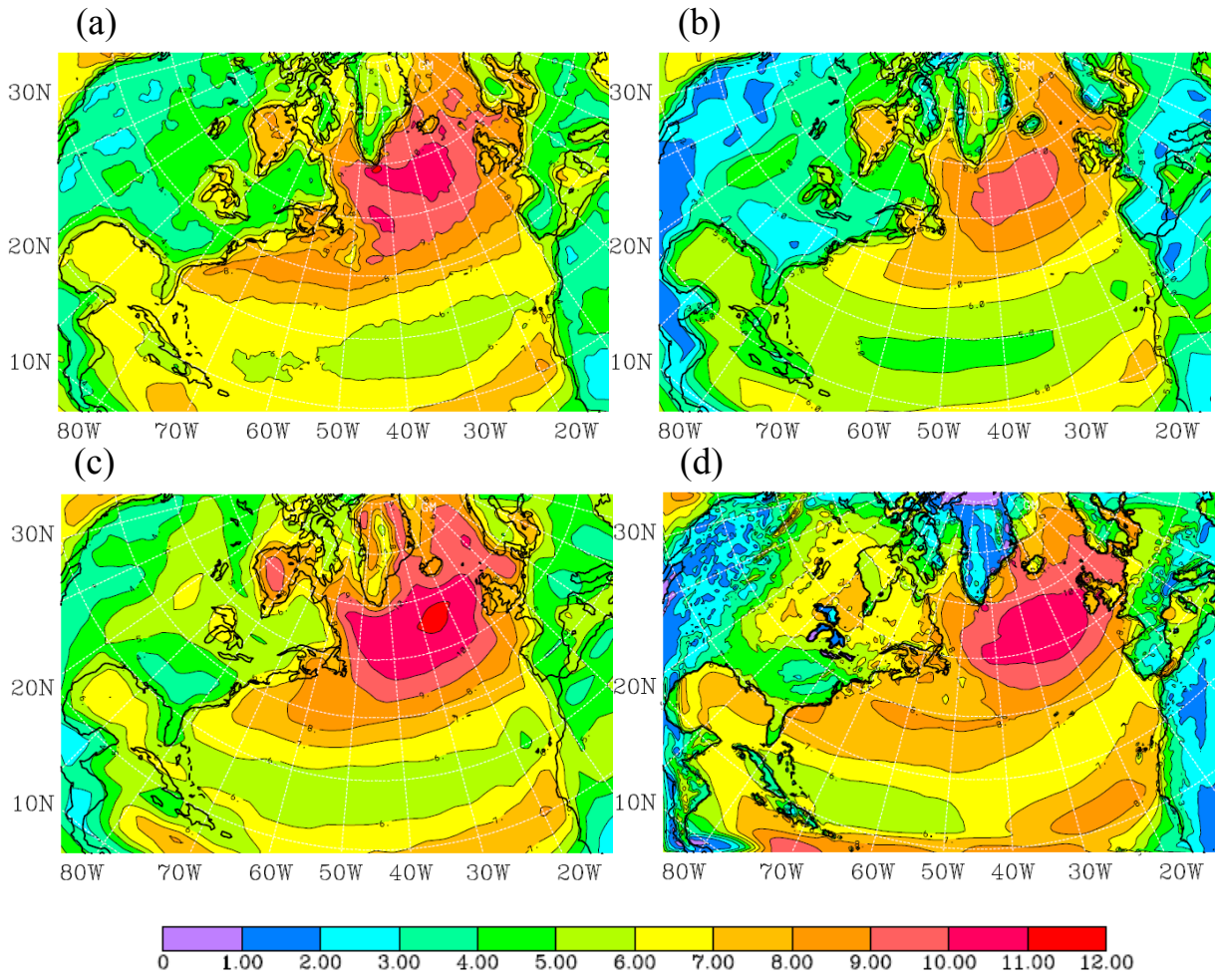

Figure 1. The seasonal mean of 6hourly 10m wind speed (a) QSCAT/NCEP (b) ERA40 (c) NCEP (d) CRCM.

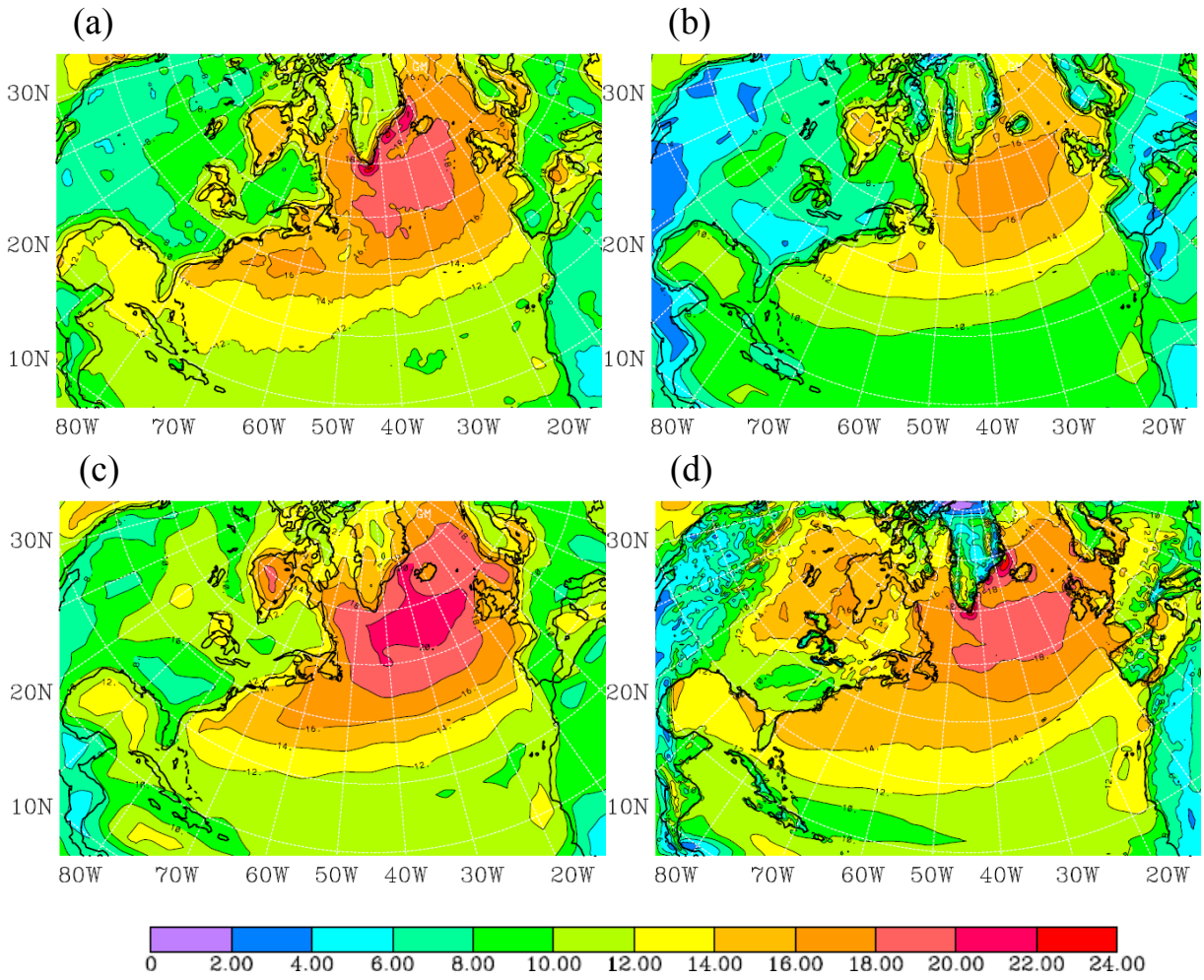

Figure 2. The mean of 10% strongest 6hourly 10m wind speed (a) QSCAT/NCEP (b) ERA40 (c) NCEP (d) CRCM.

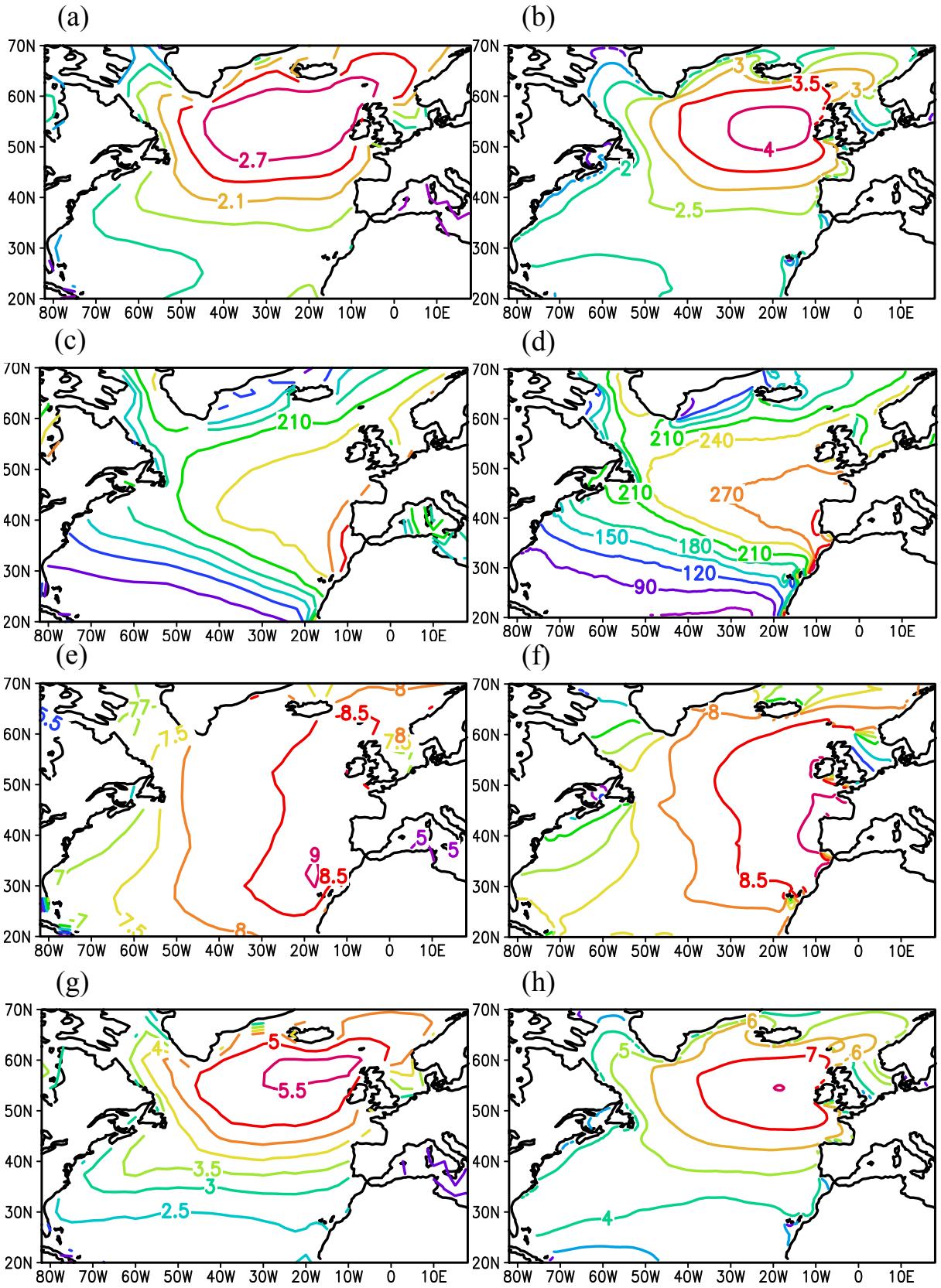

Figure 3. The seasonal mean SWH from (a)ERA40 (b) WW3; mean wave direction from (c) ERA40 (d) WW3; mean wave period from (e) ERA40 (f) WW3; and 10% strongest SWH from (g) ERA40 (h) WW3.

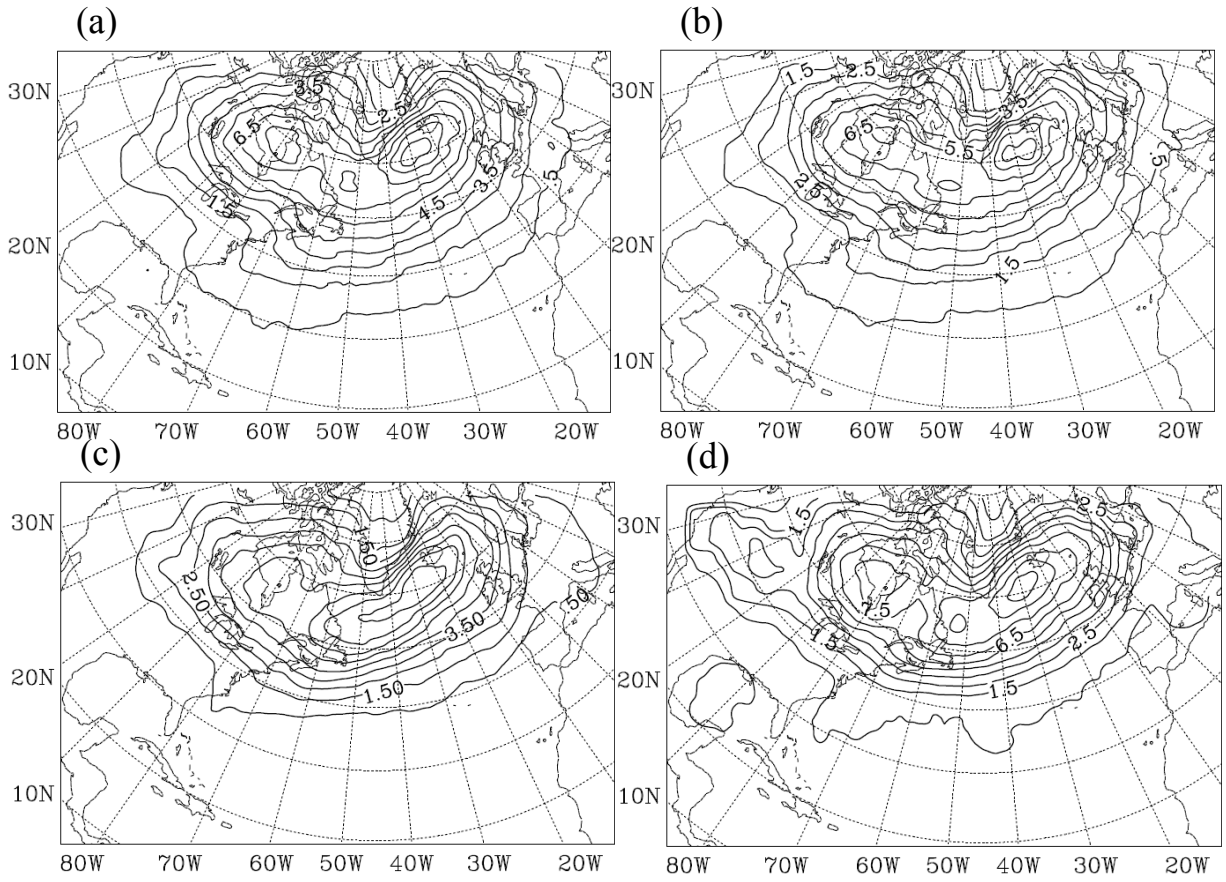

Figure 4. Track densities of total extratropical cyclones from (a) ERA40 (b) NCEP (c) CGCM3 (d) CRCM.

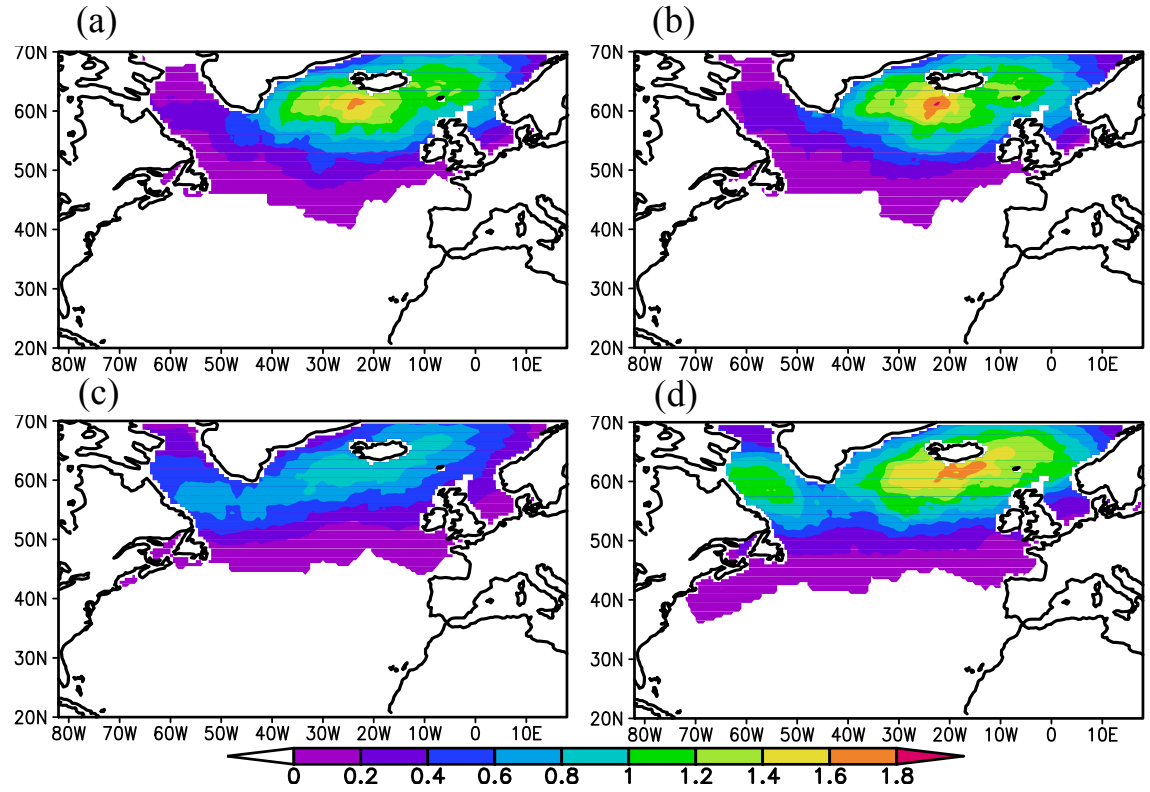

Figure 5. The track densities of strong extratropical cyclones (minimum sea level pressure ≤ 970 hPa) from (a) ERA40 (b) NCEP (c) CGCM3 (d) CRCM.

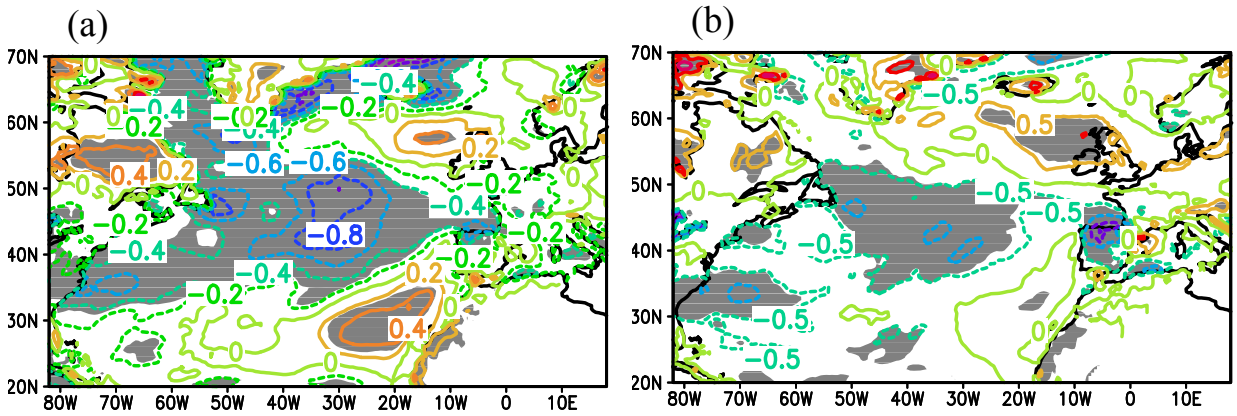

Figure 6. Difference in mean 6hourly 10m wind speed for (a) 10% strongest 6hourly 10m wind speed, and (b) for future GHG-warmed climate minus present climate by CRCM. The light shading indicates 90% significance level with Student's t-test.

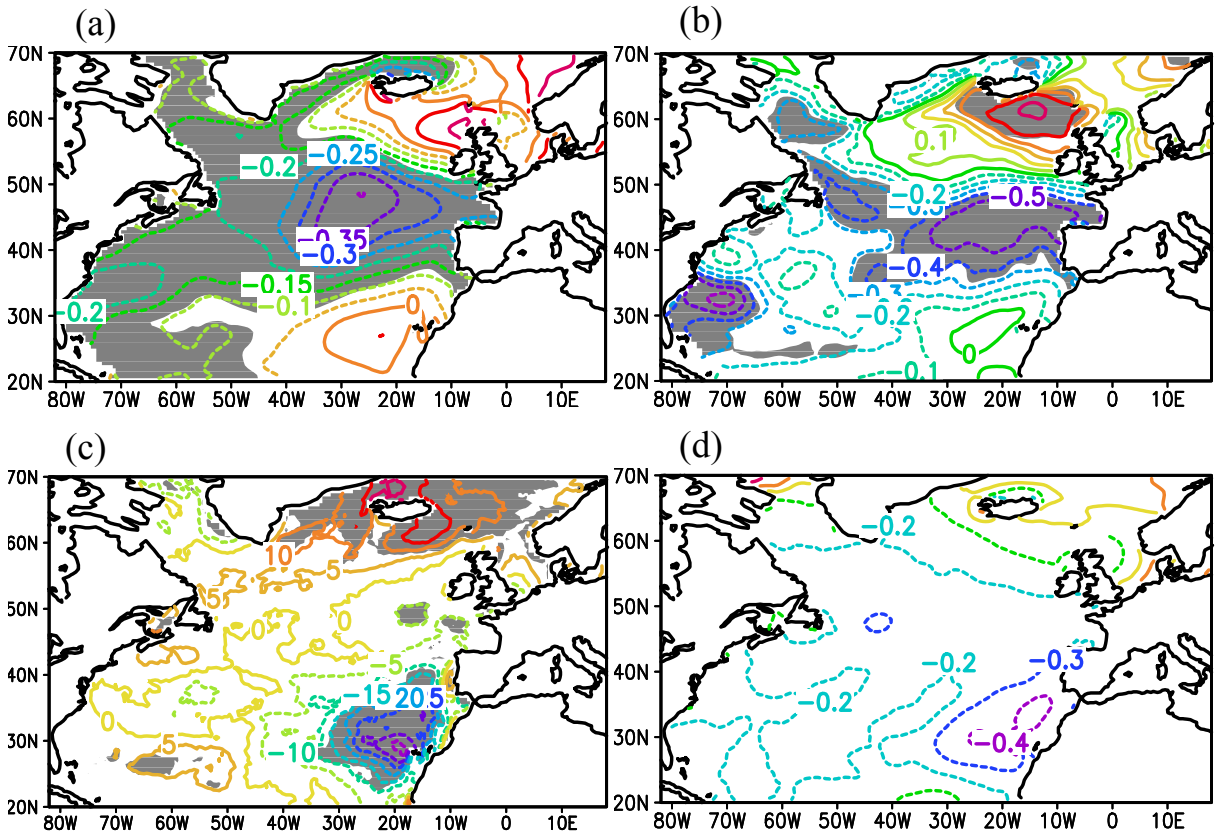

Figure 7. Difference in (a) mean SWH, (b) 10% strongest SWH, (c) mean wave direction, and (d) wave period for future GHG-warmed climate, *minus* present climate. The light shading indicates 90% significance level with Student's t-test.

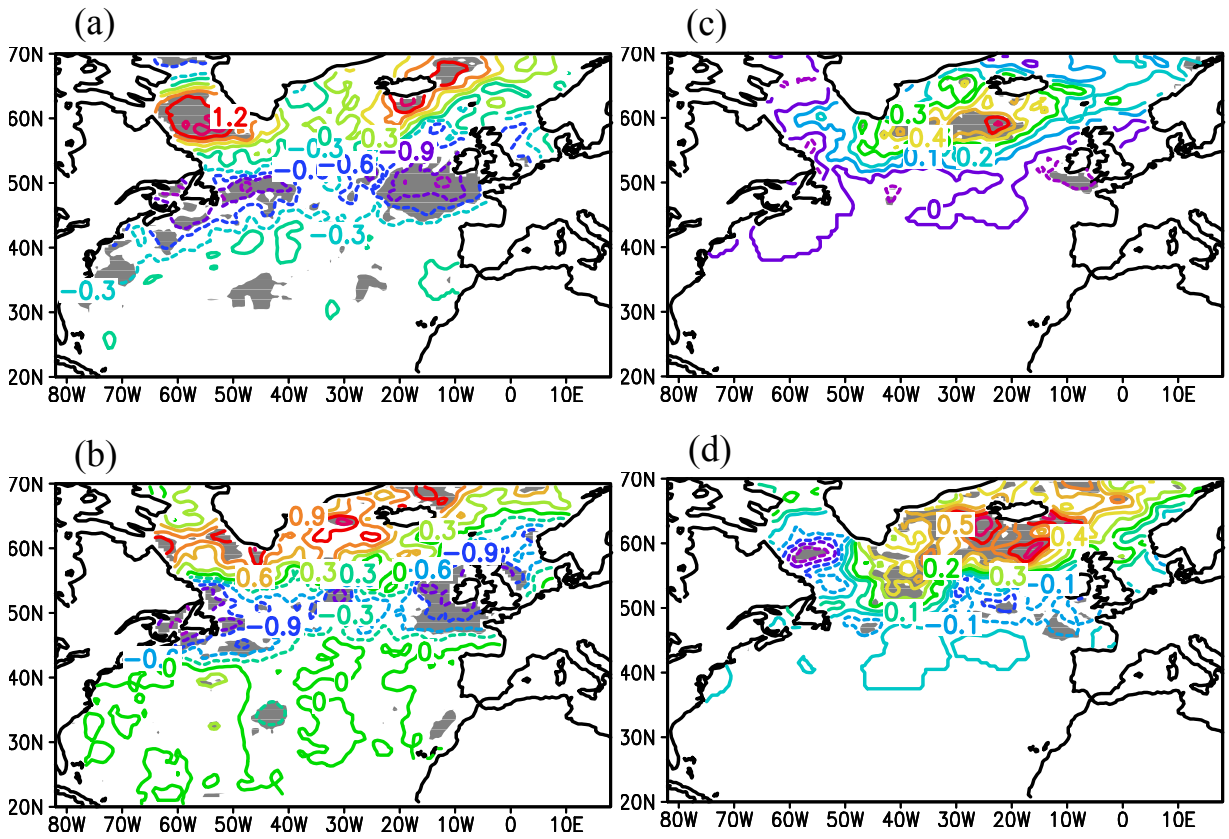

Figure 8. Difference of total cyclone track densities between future climate *minus* present climate as simulated by (a) CGCM3, (b) CRCM, (c) for minimum pressure ≤ 970 hPa as simulated by CGCM3 and (d) for minimum pressure ≤ 970 hPa as simulated by CRCM. The light shading indicates 90% significance level with the Student's t-test.